

Carbon–Nitrogen Bond Construction and Carbon–Oxygen Double Bond Cleavage on a Molecular Titanium Oxonitride: A Combined Experimental and Computational Study

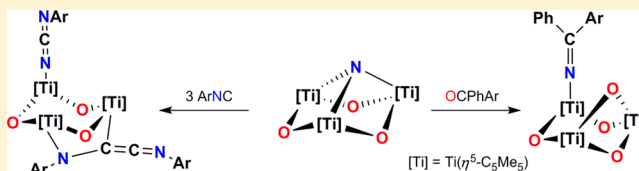
Jorge J. Carbó,^{*,†} Diego García-López,[†] Octavio González-del Moral,[‡] Avelino Martín,[‡] Miguel Mena,[‡] and Cristina Santamaría^{*,‡}

[†]Departament de Química Física i Inorgànica, Universitat Rovira i Virgili, Campus Sescelades. C/Marcel·lí Domingo, s/n. 43007 Tarragona, Spain

[‡]Departamento de Química Inorgànica, Universidad de Alcalá, Campus Universitario. 28871 Alcalá de Henares-Madrid, Spain

Supporting Information

ABSTRACT: New carbon–nitrogen bonds were formed on addition of isocyanide and ketone reagents to the oxonitride species $[\{\text{Ti}(\eta^5\text{-C}_5\text{Me}_5)(\mu\text{-O})\}_3(\mu_3\text{-N})]$ (**1**). Reaction of **1** with XylNC (Xyl = 2,6-Me₂C₆H₃) in a 1:3 molar ratio at room temperature leads to compound $[\{\text{Ti}(\eta^5\text{-C}_5\text{Me}_5)(\mu\text{-O})\}_3(\mu\text{-XylNCCNXyl})(\text{NCNXyl})]$ (**2**), after the addition of the nitrido group to one coordinated isocyanide and the carbon–carbon coupling of the other two isocyanide molecules have taken place. Thermolysis of **2** gives $[\{\text{Ti}(\eta^5\text{-C}_5\text{Me}_5)(\mu\text{-O})\}_3(\text{XylINCNXyl})(\text{CN})]$ (**3**) where the heterocumulene [XylNCCNXyl] moiety and the carbodiimido [NCNXyl] fragment in **2** have undergone net transformations. Similarly, *tert*-butyl isocyanide (*t*BuNC) reacts with the starting material **1** under mild conditions to give the paramagnetic derivative $[\{\text{Ti}_3(\eta^5\text{-C}_5\text{Me}_5)(\mu\text{-O})_3(\text{NCN}t\text{Bu})\}_2(\mu\text{-CN})_2]$ (**4**). However, compound **1** provides the oxo ketimide derivatives $[\{\text{Ti}_3(\eta^5\text{-C}_5\text{Me}_5)(\mu\text{-O})_4\}(\text{NCRPh})]$ [R = Ph (**5**), *p*-Me(C₆H₄) (**6**), *o*-Me(C₆H₄) (**7**)] upon reaction with benzophenone, *p*-methylbenzophenone, and *o*-methylbenzophenone, respectively. In these reactions, the carbon–oxygen double bond is completely ruptured, leading to the formation of a carbon–nitrogen and two metal–oxygen bonds. The molecular structures of complexes **2–4**, **6**, and **7** were determined by single-crystal X-ray diffraction analyses. Density functional theory calculations were performed on the incorporation of isocyanides and ketones to the model complex $[\{\text{Ti}(\eta^5\text{-C}_5\text{H}_5)(\mu\text{-O})\}_3(\mu_3\text{-N})]$ (**1H**). The mechanism involves the coordination of the substrates to one of the titanium metal centers, followed by an isomerization to place those substrates *cis* with respect to the apical nitrogen of **1H**, where carbon–nitrogen bond formation occurs with a low-energy barrier. In the case of aryl isocyanides, the resulting complex incorporates additional isocyanide molecules leading to a carbon–carbon coupling. With ketones, the high oxophilicity of titanium promotes the unusual total cleavage of the carbon–oxygen double bond.



INTRODUCTION

Carbon–carbon and carbon–hydrogen bond formation processes, involving organometallic complexes, have been known for decades. Elements such Pd or Rh are responsible for industrially important catalytic procedures such hydrogenation, hydroformylation, and others. In the last years, carbon–heteroatom (C–X, X = N, O, S, Si, and B) bond formation studies have focused most of the emerging catalytic methodologies. For example, nowadays the synthesis of amines, basic components for both chemical industry and organic chemistry, is one of the most active research fields.^{1,2}

The nitrido functionality has been very often utilized to promote the carbon–nitrogen bond formation due to the dual nature of this functionality as nucleophile or electrophile, depending on the metal, its oxidation state, and the ancillary ligands.³ Transition metal complexes containing metal–nitrogen multiple bonds have been therefore subject of intensive research for the last two decades. Terminal nitrido functionalities usually implicate group 6–8 metals,^{3a–g,4} while the μ_n -

nitrido moiety bridging to two or more metal centers is typical in polynuclear structures of early transition elements.^{3i,5}

In this field, our group has reported the synthesis of the μ_3 -nitride complex $[\{\text{Ti}(\eta^5\text{-C}_5\text{Me}_5)(\mu\text{-O})\}_3(\mu_3\text{-N})]$ (**1**) through ammonia activation promoted by the titanium μ_3 -alkylidyne complexes $[\{\text{Ti}(\eta^5\text{-C}_5\text{Me}_5)(\mu\text{-O})\}_3(\mu_3\text{-CR})]$ [R = H, Me], highlighting a marked cooperative effect between the three titanium atoms.⁶ In this paper we demonstrate, experimentally and theoretically, that the nitride species $[\{\text{Ti}(\eta^5\text{-C}_5\text{Me}_5)(\mu\text{-O})\}_3(\mu_3\text{-N})]$ (**1**) can promote carbon–nitrogen bond formation processes by addition of isocyanide and ketone reagents, resulting in the latter case, in complete cleavage of the carbon–oxygen double bond.

Received: April 28, 2015

Published: September 14, 2015

EXPERIMENTAL SECTION

General Procedures. All work was performed under anaerobic and anhydrous conditions by using Schlenk-line and glovebox techniques. Solvents were carefully dried from the appropriate drying agents and distilled prior to use. XylNC (Xyl = 2,6-Me₂C₆H₃) was purchased from Fluka and dried in vacuum before use. tBuNC was purchased from Aldrich and used as received. Benzophenones were purchased from Aldrich and used sublimed. [Ti(η⁵-C₅Me₅)(μ-O)]₃(μ₃-N) (1) was synthesized according to the published procedures.⁶ Elemental analysis (C, H, N) were performed with a Leco CHNS-932. NMR spectra were recorded on Varian NMR System spectrometers: Unity-300 or Mercury-VX. Trace amounts of protonated solvents or carbon of the solvent were used as references, and chemical shifts are reported relative to tetramethylsilane. Infrared spectra were acquired for samples in KBr pellets on a Fourier transform infrared PerkinElmer SPECTRUM 2000 spectrophotometer. Mass spectrometry analyses (Electron Impact, EI) were conducted at 70 eV on a Thermo Scientific ITQ 900 spectrometer.

Preparation of [Ti(η⁵-C₅Me₅)(μ-O)]₃(μ-XylNCCNXYl)(NCCNXYl) (2). A solution of 0.20 g (0.33 mmol) of complex 1, 0.13 g (0.99 mmol) of 2,6-dimethylphenylisocyanide, and 30 mL of hexane was prepared in a 100 mL Schlenk vessel. The solution was left stirring at room temperature, turning the color from green to black, and forming a black precipitate after 2 d. The solid of 2 was isolated by filtration and then dried (0.11 g, 33%). IR (KBr, cm⁻¹): $\bar{\nu}$ = 2908 (m), 2855 (m), 2185 (m), 2113 (s), 1913 (s), 1590 (m), 1508 (m), 1453 (m), 1375 (m), 1261 (m), 1221 (m), 1139 (m), 1067 (w), 1026 (m), 799 (m), 748 (s), 701 (s), 624 (m), 610 (m), 561 (m), 546 (m), 511 (w), 493 (m), 422 (m), 381 (w); ¹H NMR (C₆D₆, 300 MHz, 298 K): δ = 1.98 (very broad, 42H, 2C₅Me₅ + (2,6-Me₂C₆H₃)NC=CN(2,6-Me₂C₆H₃)), 2.18 (s, 15H, C₅Me₅), 2.64 (s, 6H, (2,6-Me₂C₆H₃)NCN), 6.72–6.96 (br, 6H, (2,6-Me₂C₆H₃)NCCN(2,6-Me₂C₆H₃)), 7.07–7.10 (3H, (2,6-Me₂C₆H₃)NCN); ¹H NMR (C₇D₈, 300 MHz, 233 K): δ = 1.80 (s, 15H, C₅Me₅), 1.92 (s, 6H, XylNC=CN(2,6-Me₂C₆H₃)), 2.02 (s, 18H, C₅Me₅ + (2,6-MeMeC₆H₃)NC=CNXYl), 2.20 (s, 15H, C₅Me₅), 2.25 (s, 3H, (2,6-MeMeC₆H₃)NC=CNXYl), 2.64 (s, 6H, (2,6-Me₂C₆H₃)NCN), 6.72–6.96 (br, 6H, (2,6-Me₂C₆H₃)NCCN(2,6-Me₂C₆H₃)), 7.07–7.10 (3H, (2,6-Me₂C₆H₃)NCN); ¹³C{¹H} NMR (C₆D₆, 75 MHz, 298 K): δ = 11.6, 12.2 (C₅Me₅), 19.3 ((2,6-Me₂C₆H₃)NCCN(2,6-Me₂C₆H₃)), 19.9 (2,6-Me₂C₆H₃)NCN, 124.3, 124.6 (C₅Me₅), 121.5–132.0 ((2,6-Me₂C₆H₃)NCN + (2,6-Me₂C₆H₃)NCCN(2,6-Me₂C₆H₃)), 141.1 ((2,6-Me₂C₆H₃)NCN), not detected ((2,6-Me₂C₆H₃)NCCN(2,6-Me₂C₆H₃)); EI mass spectrum: *m/z* (%) 611 (4) [M-(XylNC)-(XylNCCNXYl)]⁺, 477 (22) [M-(XylNC)-(XylNCCNXYl)-(C₅Me₅)]⁺, 341 (14) [M-(XylNC)-(XylNCCNXYl)-2(C₅Me₅)]⁺; Anal. Calcd (%) for C₅₇H₇₂N₄O₃Ti₃ (1004.81): C, 68.13; H, 7.22; N 5.58; found: C, 67.99; H, 7.16; N 6.15.

Thermolysis of Complex 2. Twenty mg (0.02 mmol) of 2 was dissolved in 0.6 mL of toluene-*d*₆ in an NMR tube with Young valve. The solution was heated at 150 °C for 4 d. The solution initially wine-red turns dark orange, from which [Ti(η⁵-C₅Me₅)(μ-O)]₃(μ-XylNCCNXYl)(CN) (3) is isolated as a brownish-yellow crystalline solid. IR (KBr, cm⁻¹): $\bar{\nu}$ = 2910 (m), 2113 (m), 1602 (m, C=N), 1572 (m, C=N), 1493 (w), 1468 (m), 1440 (m), 1374 (m), 1283 (m), 1166 (m), 1068 (w), 1026 (m), 775 (vs), 760 (vs), 688 (vs), 533 (m), 466 (w), 421 (m), 373 (w); ¹H NMR (C₆D₆, 300 MHz, 298 K): δ = 1.88 (s, 6H, 2,6-Me₂C₆H₃), 1.90 (s, 6H, 2,6-Me₂C₆H₃), 2.00 (s, 30H, C₅Me₅), 2.07 (s, 15H, C₅Me₅), 6.60–7.10 (6H, 2,6-Me₂C₆H₃); ¹³C{¹H} NMR (C₆D₆, 75 MHz, 298 K): δ = 11.7, 12.5 (C₅Me₅), 20.4, 21.5 (2,6-Me₂C₆H₃), 123.5, 123.8 (C₅Me₅), 121.6–143.3 ((2,6-Me₂C₆H₃)NCN(2,6-Me₂C₆H₃)), 154.8 (XylNCCNXYl), 176.3 (CN); Anal. Calcd (%) for C₄₈H₆₃N₃O₃Ti₃ (873.62): C, 65.98; H, 7.27; N 4.81; found: C, 66.58; H, 7.08; N 4.31.

Preparation of [Ti₃(η⁵-C₅Me₅)₃(μ-O)₃(NCNtBu)₂(μ-CN)₂] (4). Although the synthesis of this complex was performed in toluene several times, and it led us to obtain suitable single crystals for the diffraction study, here we report the synthesis in hexane that leads to better yields. In a 50 mL Schlenk containing 0.20 g (0.33 mmol) of 1 and 0.08 g (0.66 mmol) of tBuNC, 25 mL of hexane was added. This

reaction mixture was allowed to stir at room temperature overnight affording a dark precipitate. The solution was filtered, and the solid was dried to give 0.13 g (56%) of 4. IR (KBr, cm⁻¹): $\bar{\nu}$ = 2965 (m), 2915 (m), 2909 (s), 2359 (m), 2208 (w), 2139 (m), 2085 (vs), 1651 (m), 1554 (w), 1493 (m), 1435 (m), 1374 (m), 1231 (m), 1072 (w), 1025 (m), 780 (vs), 698 (s), 618 (m), 470 (m), 416 (m); Anal. Calcd (%) for C₇₂H₁₀₈N₆O₆Ti₆ (1440.86): C, 60.01; H, 7.55; N 5.83; found: C, 59.61; H, 8.06; N 5.63. The effective magnetic moment of 4 was determined to be 2.58 μ_B (based on a unit formula of C₇₂H₁₀₈N₆O₆Ti₆) by the Evans NMR method on a C₅D₅N solution at 293 K (using a 300 MHz instrument with a field strength of 7.05 T).

Preparation of [Ti₃(η⁵-C₅Me₅)₃(μ-O)₄(NCPh)₂] (5). [Ti(η⁵-C₅Me₅)(μ-O)]₃(μ₃-N) (1) (0.30 g, 0.49 mmol) and Ph₂CO (0.09 g, 0.49 mmol) were placed in a 100 mL ampule with Young valve and dissolved in 30 mL of toluene. The solution was heated at 90 °C for 3 d. The dark suspension was then filtered, and the solution was dried under vacuum. Complex 5 was obtained as an oily solid that, after it was treated at high vacuum for hours, gave 0.31 g of a brown solid (Yield: 80%). IR (KBr, cm⁻¹): $\bar{\nu}$ = 2910 (m), 2854 (m), 1630 (m, N=C), 1572 (w), 1491 (m), 1442 (m), 1375 (m), 1314 (w), 1258 (m), 1174 (w), 1070 (w), 1026 (m), 905 (w), 884 (w), 790 (s), 706 (s), 626 (s), 460 (m); ¹H NMR (C₆D₆, 300 MHz, 298 K): δ = 1.99 (s, 15H, C₅Me₅), 2.07 (s, 30H, C₅Me₅), 6.8–8.0 (10H, Ph₂CN); ¹H NMR (CDCl₃, 300 MHz, 298 K): δ = 1.85 (s, 15H, C₅Me₅), 1.99 (s, 30H, C₅Me₅), 7.12–7.84 (10H, Ph₂CN); ¹³C{¹H} NMR (C₆D₆, 75 MHz, 298 K): δ = 11.5, 11.9 (C₅Me₅), 121.2, 122.2 (C₅Me₅), 126.9–139.6 (Ph)₂CN, 170.4 (Ph₂CN); ¹³C{¹H} NMR (CDCl₃, 75 MHz, 298 K): δ = 11.3, 11.6 (C₅Me₅), 121.2, 122.1 (C₅Me₅), 127.6–139.0 (Ph)₂CN, 170.2 (Ph₂CN); EI mass spectrum: *m/z* (%) 613 (14) [M–NCPh]⁺; Anal. Calcd (%) for C₄₃H₅₅NO₄Ti₃ (793.50): C, 65.09; H, 6.99; N 1.77; found: C, 64.93; H, 6.89; N 1.98.

Preparation of [Ti₃(η⁵-C₅Me₅)₃(μ-O)₄(NC(4-MeC₆H₄)Ph)] (6). A solution containing 0.30 g (0.49 mmol) of [Ti(η⁵-C₅Me₅)(μ-O)]₃(μ₃-N) (1), 0.10 g (0.51 mmol) of 4-methylbenzophenone, and 30 mL of toluene was prepared in a 100 mL ampule with Young valve. The solution was left stirring and heated at 90 °C for 5 d. After filtration, the solvent was removed under vacuum, and the dark residue was extracted with 20 mL of hexane. The solution was concentrated to half volume and cooled at –20 °C, obtaining dark red crystals of complex 6 (0.21 g, 54%). IR (KBr, cm⁻¹): $\bar{\nu}$ = 2908 (s), 2854 (m), 1657 (m), 1639 (s, N=C), 1604 (m), 1576 (w), 1491 (w), 1445 (m), 1374 (m), 1276 (m), 1263 (m), 1177 (m), 1027 (m), 784 (s), 744 (s), 711 (s), 643 (s), 608 (m), 580 (m), 393 (m); ¹H NMR (C₆D₆, 300 MHz, 298 K): δ = 2.01 (s, 15H, C₅Me₅), 2.09 (s, 30H, C₅Me₅), 2.12 (s, 3H, 4-MeC₆H₄), 7.00–7.75 (9H, (4-MeC₆H₄)PhCN); ¹³C{¹H} NMR (C₆D₆, 75 MHz, 298 K): δ = 11.6, 11.9 (C₅Me₅), 21.3 (4-MeC₆H₄)PhCN, 121.2, 122.1 (C₅Me₅), 127.4–139.9 (4-MeC₆H₄)PhCN, 170.4 (4-MeC₆H₄)PhCN; EI mass spectrum: *m/z* (%) 613 (2) [M–NC(MeC₆H₄)Ph]⁺; Anal. Calcd (%) for C₄₄H₅₇NO₄Ti₃ (807.53): C, 65.44; H, 7.11; N 1.73; found: C, 65.61; H, 6.88; N 1.67.

Preparation of [Ti₃(η⁵-C₅Me₅)₃(μ-O)₄(NC(2-MeC₆H₄)Ph)] (7). Following the same method used to prepare 6, 0.30 g (0.49 mmol) of [Ti(η⁵-C₅Me₅)(μ-O)]₃(μ₃-N) (1) and 0.10 g (0.51 mmol) of 2-methylbenzophenone in 30 mL of toluene led us to obtain 0.11 g (28%) of complex 7 as deep red crystals. IR (KBr, cm⁻¹): $\bar{\nu}$ = 2909 (s), 2855 (s), 1639 (s, N=C), 1489 (w), 1444 (m), 1372 (m), 1287 (w), 1253 (m), 1024 (m), 906 (w), 751 (s), 714 (s), 628 (m), 545 (w), 506 (w), 455 (m), 395 (s); ¹H NMR (C₆D₆, 300 MHz, 298 K): δ = 2.00 (s, 15H, C₅Me₅), 2.05 (s, 30H, C₅Me₅), 2.25 (s, 3H, 2-MeC₆H₄), 7.00–7.75 (9H, (2-MeC₆H₄)PhCN); ¹³C{¹H} NMR (C₆D₆, 75 MHz, 298 K): δ = 11.5, 11.9 (C₅Me₅), 20.7 (2-MeC₆H₄)PhCN, 121.3, 122.2 (C₅Me₅), 125.4–141.6 (2-MeC₆H₄)PhCN, 171.7 (2-MeC₆H₄)PhCN; EI mass spectrum: *m/z* (%) 613 (5) [M–NC(MeC₆H₄)Ph]⁺; Anal. Calcd (%) for C₄₄H₅₇NO₄Ti₃ (807.53): C, 65.44; H, 7.11; N 1.73; found: C, 65.87; H, 7.21; N 1.70.

Crystal Structure Determination of Complexes 2, 3, 4, 6, and 7. Crystals were grown by slow evaporation at room temperature of saturated hexane (2, 6, 7) or toluene (3, 4) solutions. Then crystals were removed from the Schlenks and covered with a layer of a viscous perfluoropolyether (FomblinY). A suitable crystal was selected with

Table 1. Experimental Data for the X-ray Diffraction Studies on 2, 3, 4, 6, and 7

	2	3	4	6	7
formula	C ₅₇ H ₇₂ N ₄ O ₃ Ti ₃	C ₄₈ H ₆₃ N ₃ O ₃ Ti ₃ · C ₇ H ₈	C ₇₂ H ₁₀₈ N ₆ O ₆ Ti ₆ · 2C ₇ H ₈	C ₄₄ H ₅₇ N ₄ O ₃ Ti ₃	C ₄₄ H ₅₇ N ₄ O ₃ Ti ₃
M	1004.89	965.84	1625.3	807.61	807.61
T [K]	200(2)	200(2)	200(2)	200(2)	200(2)
λ [Å]	0.710 73	0.710 73	0.710 73	0.710 73	0.710 73
crystal system	monoclinic	triclinic	monoclinic	monoclinic	monoclinic
space group	P2 ₁ /c	P $\bar{1}$	P2 ₁ /c	P2 ₁ /c	P2 ₁ /n
a [Å]; α [deg]	15.324(2)	12.198(2); 94.04(2)	15.883(5)	12.857(2)	12.806(1)
b [Å]; β [deg]	14.140(7); 90.20(2)	12.518(3); 94.28(2)	16.313(6); 115.98(1)	21.714(5); 121.82(2)	21.745(3); 103.12(1)
c [Å]; γ [deg]	25.099(9)	17.154(3); 104.02(1)	18.762(2)	17.775(4)	15.429(1)
V [Å ³]	5439(4)	2523.6(9)	4370(2)	4216(1)	4184.1(8)
Z	4	2	2	4	4
ρ _{calcd} [g cm ⁻³]	1.227	1.271	1.235	1.272	1.282
μ [mm ⁻¹]	0.475	0.512	0.574	0.595	0.6
F(000)	2128	1024	1724	1704	1704
crystal size [mm ³]	0.32 × 0.13 × 0.06	0.36 × 0.30 × 0.25	0.30 × 0.24 × 0.15	0.37 × 0.35 × 0.35	0.43 × 0.27 × 0.21
θ range [deg]	3.02–25.01	3.05–27.50	3.08–27.63	2.99–27.57	3.12–27.51
index ranges	–18 to 18, –16 to 16, –29 to 29	–15 to 15, –16 to 16, –22 to 22	–20 to 18, –21 to 21, 0 to 24	–16 to 16, –28 to 28, –23 to 23	–16 to 15, –28 to 28, 0 to 20
reflections collected	70 143	96 288	92 774	77 938	88 320
unique data	9515 (R _{int} = 0.178)	11 593 (R _{int} = 0.099)	10 089 (R _{int} = 0.227)	9549 (R _{int} = 0.114)	9496 (R _{int} = 0.105)
reflections [I > 2σ(I)]	6051	8137	3924	6608	4702
goodness-of-fit on F ²	1.178	1.093	0.887	1.223	1.038
final R indices ^a [I > 2σ(I)]	R1 = 0.081 wR2 = 0.188	R1 = 0.047 wR2 = 0.108	R1 = 0.072 wR2 = 0.138	R1 = 0.087 wR2 = 0.188	R1 = 0.071 wR2 = 0.150
R indices ^a (all data)	R1 = 0.142 wR2 = 0.232	R1 = 0.085 wR2 = 0.130	R1 = 0.175 wR2 = 0.181	R1 = 0.132 wR2 = 0.212	R1 = 0.171 wR2 = 0.188
largest diff peak/hole [e ⁻ Å ⁻³]	0.71/–0.789	0.631/–0.525	0.580/–0.584	1.034/–0.684	0.455/–0.553

$$^a R1 = \frac{\sum ||F_o| - |F_c||}{\sum |F_o|}, \text{ and } wR2 = \left\{ \frac{\sum w(F_o^2 - F_c^2)^2}{\sum w(F_o^2)^2} \right\}^{1/2}.$$

the aid of a microscope, attached to a glass fiber, and immediately placed in the low-temperature nitrogen stream of the diffractometer. The intensity data sets were collected at 200 K on a Bruker-Nonius KappaCCD diffractometer equipped with an Oxford Cryostream 700 unit. Crystallographic data for all complexes are presented in Table 1. The structures were solved, by use of the WINGX package,⁷ by direct methods (SHELXS-97 for complexes 2, 4, 6, and 7; SHELXS-2013 for 3)⁸ and refined by least-squares against F² (SHELXL-97 for complexes 2, 6, and 7; SHELXL-2014 for 3 and 4).⁸

All crystals diffracted weakly, and only data collections up to θ = 25.01° could be performed for crystals of 2. Complex 3 crystallized with one disordered molecule of toluene, while molecules of 4 were solvated with two molecules of toluene. All the hydrogen atoms were positioned geometrically and refined by using a riding model. All non-hydrogen atoms were anisotropically refined.

By using the corresponding Shelxl's PART commands⁸ and FVAR variables, two positions for the disordered molecule of toluene in 3 were refined with 36.8% and 63.2% occupancy, respectively.

However, molecules of complex 4 presented disorder in the C43, C44, and C45 carbon atoms of the *tert*-butyl group, and two positions were refined for each atom with 53% and 48% occupancy, respectively. Additionally, it was not possible to assign unambiguously the scattering factors for the atoms bridging Ti(1) and Ti(2)a; thus, the cyanide bridging atoms (CN atoms in Figure 7) were refined with the aid of the EXYZ and EADP Shelxl's commands to obtain occupancies of 59% and 41%, respectively. Additional crystallographic information is available in the Supporting Information.

Computational Details. All calculations were performed with the Gaussian09 series of programs⁹ within the framework of the density functional theory (DFT)¹⁰ using the B3LYP functional.¹¹ A quasi-relativistic effective core potential operator was used to represent the 10 innermost electrons of the Ti atom.¹² The basis set for Ti atoms was that associated with the pseudopotential,¹² with a standard double-

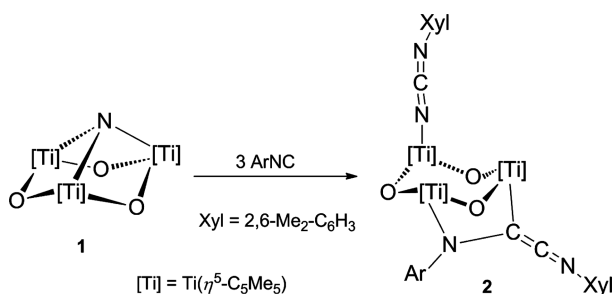
ξ LANL2DZ contraction.⁹ The 6-31G(d) basis set was used for C, N, and O atoms,¹³ and the 6-31G-basis set was used for the hydrogens.¹³ Such a computational level has been successfully employed in the study of the reactivity of these⁶ and other¹⁴ titanium molecular oxides, including quantitative agreement with Arrhenius activation energies.^{14c} For example, we recently compared the potential free energy surfaces for the thioether oxidation by di- and tetratitanium-substituted molecular oxides derived from kinetics data and DFT calculations finding differences of 2–10 kJ·mol⁻¹ for relative energies and of ~12 kJ·mol⁻¹ for energy barriers.^{14d} Geometry optimizations were performed without any symmetry restrictions, and all stationary points were optimized with analytical first derivatives. Transition states were characterized by single imaginary frequency, whose normal mode corresponded to the expected motion. The only exception is the transition state TS_{AA'} for aryl isocyanide, for which we found a residual imaginary frequency corresponding to one cyclopentadienyl rotation. The solvent effect of hexane was evaluated with the self-consistent reaction field approach, by means of the integral equation formalism polarizable continuum model (IEFPCM),¹⁵ where optimized structures in gas phase were employed. The Gibbs free-energy in solution was employed for discussion, where the translational entropy was evaluated with the method developed by Whitesides et al.,¹⁶ following the procedure adapted by Sakaki et al.¹⁷ In this approach we used a hexane concentration of 0.6605 g/cm³¹⁸ and molecular volume for hexane solvent of 11.33 × 10⁻²³ cm³ per molecule.¹⁹ The employed equations are described in detail in the Supporting Information.

RESULTS AND DISCUSSION

The addition of 3 equiv of XylNC (Xyl = 2,6-Me₂C₆H₃) to the oxonitride species [$\{\{\eta^5\text{-C}_5\text{Me}_5\}\text{Ti}(\mu\text{-O})\}_3(\mu_3\text{-N})\}$] (1) in hexane at room temperature generates a dark red solution from which compound [$\{\text{Ti}(\eta^5\text{-C}_5\text{Me}_5)(\mu\text{-O})\}_3(\mu\text{-$

$\text{XylNCCNXYl}(\text{NCNXYl})$ (**2**) is isolated as a black microcrystalline solid in moderate yield (Scheme 1). When followed

Scheme 1. Reaction of **1** with XylNC



by ^1H NMR spectroscopy in benzene- d_6 , the reaction between **1** and XylCN, in 1:1 or 1:2 ratio, gave the same compound **2**. The unambiguous identity of **2** as the product of the incorporation of three molecules of arylisocyanide could only be established by performing a single-crystal X-ray diffraction study.

In this sense, the ^1H NMR spectrum of **2** in C_6D_6 or C_7D_8 , for the crystals studied by X-ray diffraction, was intriguing as it seemed to suggest the product decomposition or the existence of an intractable mixture of products (Figure 1, upper). For instance, the ^1H NMR spectrum showed as a more remarkable feature a very broad signal at δ 1.98, which integral corresponded to 42 protons. Additionally, two resonances at δ 2.18 and 2.64 assigned to a $\eta^5\text{-C}_5\text{Me}_5$ ligand and two methyl groups, respectively, were observed. Then we decided to register the ^1H NMR spectrum in C_7D_8 at 233 K (Figure 1,

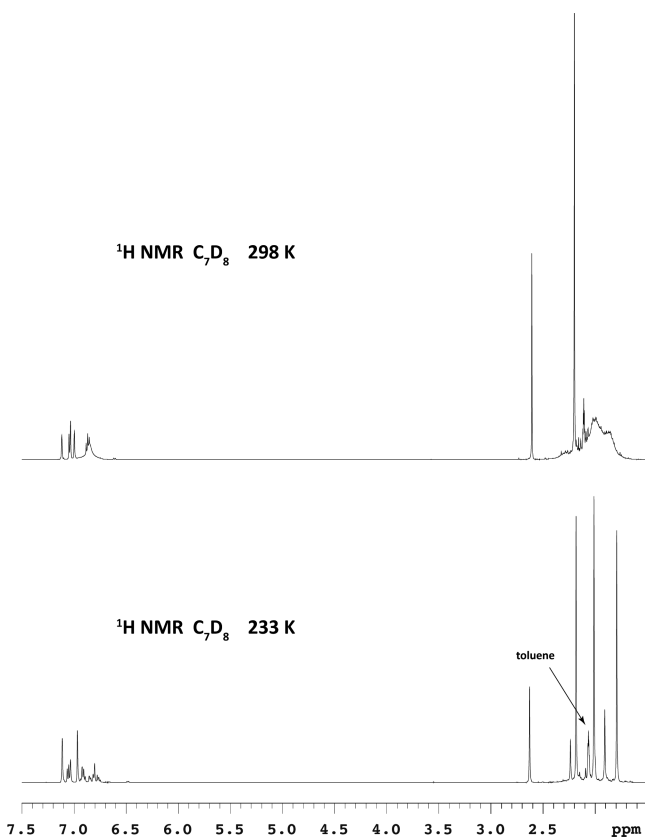
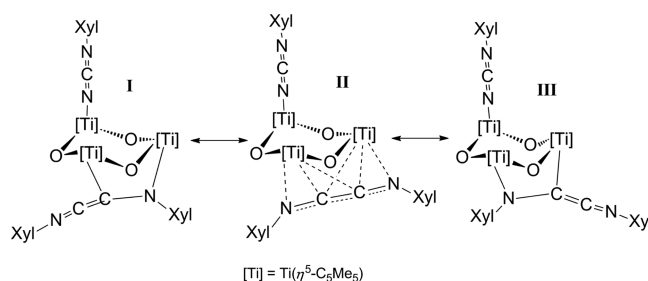


Figure 1. ^1H NMR of complex **2** recorded in C_7D_8 .

lower); it presented well-defined resonances coherent with the structural situation determined by X-ray diffraction. The three signals at δ 1.80, 2.02, and 2.18 indicated the nonequivalence of the three pentamethylcyclopentadienyl ligands of complex **2**. The rest of the resonances (see Experimental Section) were able to assign to the heterocumulene $\mu\text{-[XylNCCNXYl]}$ and carbodiimido $[\text{NCNXYl}]$ fragments.

According with these data, the broad signal found at 1.98 ppm in the ^1H NMR spectrum at room temperature might indicate a dynamic behavior (Scheme 2) of the heterocumulene $[\text{XylNCCNXYl}]$ fragment on the titanium metal centers of the molecular oxide $[\text{Ti}_3\text{O}_3]$.

Scheme 2



The $^{13}\text{C}\{^1\text{H}\}$ NMR spectrum in C_6D_6 registered only four signals corresponding to the pentamethylcyclopentadienyl ligands, two at low field for the ipso carbon atoms at δ 124.3 and 124.6 (broad signal) and the other two at high field at δ 11.6 and 12.2 (broad signal) for the methyl groups in agreement with the rapid interchange of the heterocumulene fragment. Also noteworthy is the chemical shift of the sp-hybridized carbon of the carbodiimido moiety (δ 141.1).^{20,21} Additionally, the IR spectrum shows bands at 2185, 2113, 1590, and 1508 cm^{-1} , characteristic of this ligand.^{3g,21}

The solid-state structure of $[\{\text{Ti}(\eta^5\text{-C}_5\text{Me}_5)(\mu\text{-O})\}_3(\mu\text{-XylNCCNXYl})(\text{NCNXYl})]$ (**2**) and selected distances and angles are shown in Figure 2. The X-ray structure of this compound may be described as a surface, comprising the three titanium atoms and the three oxygen atoms, with a heterocumulene $[\text{XylNCCNXYl}]$ moiety above the $[\text{Ti}_3\text{O}_3]$ ring, bridging two titanium atoms, and a carbodiimido fragment $[\text{XylNCCN}]$ on the other titanium atom below, as already outlined for bonding systems I and III in Scheme 2.

Compounds of the type $[(\text{L})\text{M}-\text{NCNR}]$ ($\text{R} = \text{alkyl, aryl, ...}$) are well-known.^{3g,21,22} The $\text{Ti}(3)-\text{N}(1)$ distance (2.004(6) Å) is within the known values for titanium-carbodiimide complexes as $[\text{Ti}(\eta^5\text{-C}_5\text{H}_5)_2(\text{N}=\text{C}=\text{NPh})_2]$ (2.002(4) and 1.985(5) Å)^{21a} or $[\text{Ti}(\text{N}_2\text{N}^{\text{R}})(\text{NCNR}')(\text{NPh}_2)]$ (1.973(6) Å: $\text{R} = \text{Py}$, $\text{R}' = t\text{Bu}$; 1.970(3) Å: $\text{R} = \text{Me}$, $\text{R}' = \text{Xyl}$).^{21b} The distances for $\text{C}(71)-\text{N}(1)$ (1.183(8) Å) and $\text{C}(71)-\text{N}(7)$ (1.251(9) Å) and the angle $\text{N}(1)-\text{C}(71)-\text{N}(7)$ ($171.0(7)^\circ$) are within the known ranges.²¹

The other point of interest in **2** is the heterocumulene fragment $[\text{XylNCCNXYl}]$. To the best of our knowledge, there is a unique structure in the bibliography with a similar isocyanide coupling reported by Teuben et al. for the complex $[\{\text{Ti}(\eta^5\text{-C}_5\text{Me}_5)\text{Cl}_2\}_2\{\mu\text{-N}_2\text{C}_2(2,6\text{-Me}_2(\text{C}_6\text{H}_3))_2\}]$, but the structural disposition of the heterocumulene ligand is clearly different.²³

As can be seen in Figure 2, the interaction of the heterocumulene fragment with the Ti_3O_3 moiety leads to the formation of a five-membered ring, where the distance $\text{N}(6)-$

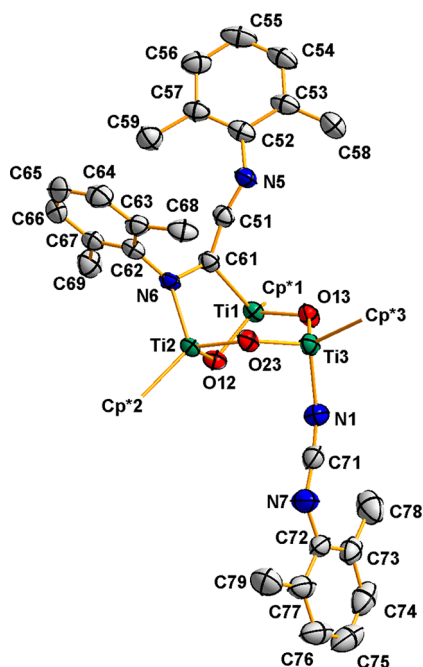


Figure 2. Ortep drawing of the molecular structure of complex 2. Thermal ellipsoids at 50% of probability. Pentamethylcyclopentadienyl groups and hydrogen atoms were omitted for clarity. Averaged selected lengths (Å) and angles (deg): Ti–O 1.84(3), C(51)–N(5) 1.236(7), C(51)–C(61) 1.324(8), C(52)–N(5) 1.427(8), C(61)–N(6) 1.447(7), C(61)–Ti(1) 2.188(6), C(61)–Ti(2) 2.671(6), C(62)–N(6) 1.415(7), C(71)–N(1) 1.183(8), C(71)–N(7) 1.251(9), C(72)–N(7) 1.400(9), N(1)–Ti(3) 2.004(6), N(6)–Ti(2) 1.930(4), C(51)–C(61)–N(6) 124.9(5), N(5)–C(51)–C(61) 166.8(6), C(51)–N(5)–C(52) 133.7(5), C(61)–N(6)–Ti(2) 103.6(3), N(6)–C(61)–Ti(1) 118.1(4), C(71)–N(7)–C(72) 136.6(7), N(1)–C(71)–N(7) 171.0(7), C(71)–N(1)–Ti(3) 159.9(5).

C(61) bond length of 1.447(7) Å is longer than a C–N bond (sp^2 -N, 1.36 Å) and close to that reported for methylamine (sp^3 -N, 1.47 Å).²⁴ Additionally, the N(6)–Ti(2) of 1.930(4) Å, similar to that found for the mononuclear $[\text{Ti}(\eta^5\text{-C}_5\text{Me}_5)_3(\text{NMe}_2)_3]$ (av. 1.917(8) Å),²⁵ suggests the existence of $p\pi \rightarrow d\pi$ interaction (see DFT study below).

However, the Ti(1)–C(61) [2.188(6) Å], C(61)–C(51) [1.324(8) Å], C(51)–N(5) [1.236(7) Å], and N(5)–C(52) [1.427(8) Å] bond lengths in complex 2 are analogous to the structural parameters of the Ti–C=C=NXYl unit published by Beckhaus and co-workers in the complex $[\text{Ti}(\eta^5\text{-C}_5\text{Me}_5)_2\text{C}(\text{=NXYl})\text{C}(\text{=NXYl})\text{CH}_2\text{C}(\text{=NXYl})]$.²⁶ Additionally, the angle N(5)–C(51)–C(61) of 166.8(6)° leads to propose the existence of two double bonds around C(51), without electronic delocalization along the C(61)–N(6) bond. Finally, the molecular core $[\text{Ti}_3(\eta^5\text{-C}_5\text{Me}_5)_3\text{O}_3]$ reveals an average distance Ti–O of 1.84(3) Å and the rest of parameters in the range found for these kind of structures.²⁷

Thermolysis of a red-dark solution of 2 in C_7D_8 for 4 d at 150 °C via ^1H NMR spectroscopy revealed complete consumption of the starting complex and formation of a brownish-yellow crystal fraction at the bottom of the NMR tube. The structure of this new compound $[\{\text{Ti}(\eta^5\text{-C}_5\text{Me}_5)(\mu\text{-O})\}_3(\eta^3\text{-XylNCNXYl})(\text{CN})]$ (3) was elucidated by single-crystal X-ray diffraction.

As can be seen in Figure 3, the molecular structure of complex 3 shows a carbodiimido fragment $[\text{XyNCNXY}]$,

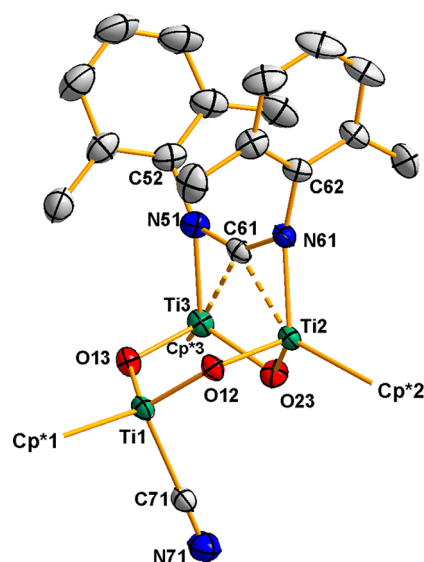


Figure 3. Simplified ORTEP drawing of the molecular structure of complex 3. Thermal ellipsoids at 50% of probability. Averaged selected lengths (Å) and angles (deg): Ti–O 1.85(4), C(52)–N(51) 1.446(3), C(61)–N(61) 1.310(3), C(61)–N(51) 1.309(3), C(61)–Ti(3) 2.174(2), C(61)–Ti(2) 2.191(2), C(62)–N(61) 1.438(3), N(71)–C(71) 1.125(3), N(51)–Ti(3) 2.062(2), N(61)–Ti(2) 2.048(2), C(71)–Ti(1) 2.176(3), N(71)–C(71)–Ti(1) 178.6(2), N(61)–C(61)–N(51) 143.4(2), C(52)–N(51)–Ti(3) 154.8(2), C(61)–N(51)–C(52) 128.4(2), C(61)–N(61)–C(62) 125.8(2), C(62)–N(61)–Ti(2) 155.4(2).

bridging two of the three metal centers, and a cyanido moiety on the third titanium atom in a syn–anti disposition with respect to the organometallic oxide fragment $[\text{Ti}_3(\eta^5\text{-C}_5\text{Me}_5)_3\text{O}_3]$. The formation of the cyanide fragment in compound 3 constitutes, to our knowledge, the first example of dearylation of an isocyanido ligand. Thus, while cyanation of metal centers via dearylation of nitrile substrates are known,²⁸ analogous processes with isocyanides CNR have not been reported.

The Ti(1)–C(71) bond length of 2.176(3) Å in the cyanido moiety is similar to those found in other cyanide complexes of titanium(IV). Also, the C(71)–N(71) bond length of 1.125(3) Å compares well to a CN triple bond, and the Ti(1)–C(71)–N(71) is almost linear $[178.6(2)^\circ]$.²⁹

Moreover, the connectivity between the $[\text{XyNCNXY}]$ moiety and the organometallic oxide resembles the only four examples reported in the literature for the coordination of carbodiimidos to $\text{W}_2(\text{OR})_6$.³⁰ Thus, the C–N bond lengths [1.309(3) and 1.310(3) Å], together with the N(61)–C(61)–N(51) angle of 143.4(2)°, are in line with an electronic delocalization along the NCN unit, similarly to the mentioned tungsten complexes.

The aromatic rings linked to N(51) and N(61) present dihedral angles of 72.1(1)° and 84.7(1)° with respect to the plane formed by the atoms N(51), Ti(3), C(61), Ti(2), and N(61). These data are consistent with the absence of π contribution from the two aromatic rings joined to the nitrogen atoms. The Ti(2)–N(61) and Ti(3)–N(51) bond lengths are in good agreement with standard Ti–N covalent bond lengths ($\Sigma_{\text{rcov}} = 2.07$ Å)³¹ with absence of multiple bonding.

Also, Ti(2)–C(61) and Ti(3)–C(61) bond distances of 2.191(2) and 2.174(2) Å, respectively, are similar to that found for Ti(1)–C(61) in complex 2. Thus, all the bond distances together with the sum of the angles ($\Sigma = 360.5^\circ$) around

C(61) leads to a planar-tetracoordinate carbon atom geometrical environment already known in the literature.³²

The NMR spectra of **3**, according with a C_s symmetry in solution, show the expected resonances for the pentamethylcyclopentadienyl ligands, and the carbodiimido and cyanido fragments (see [Experimental Section](#)). In the IR spectrum two bands appear at 1602 (m) and 1572 (m) cm^{-1} , corresponding to the carbodiimido $\text{C}=\text{N}$ stretching vibrations. Additionally, a band at 2113(m) cm^{-1} can be assigned to the terminal cyanido group.²⁹

To investigate the incorporation of the isocyanides to the molecular titanium oxonitride and the formation new carbon–nitrogen bonds, we performed DFT calculations on the isocyanides RNC ($\text{R} = \text{Ph}$ and Me) and the model molecular oxonitride $[\text{Ti}(\eta^5\text{-C}_5\text{H}_5)(\mu\text{-O})_3(\mu_3\text{-N})]$ (**1H**). We could find different types of minima corresponding to the incorporation of one (**A** and **B**), two (**C** and **D**), and three isocyanides to **1H**. [Figure 4](#) and [Scheme 3](#) show the Gibbs free-energy variation

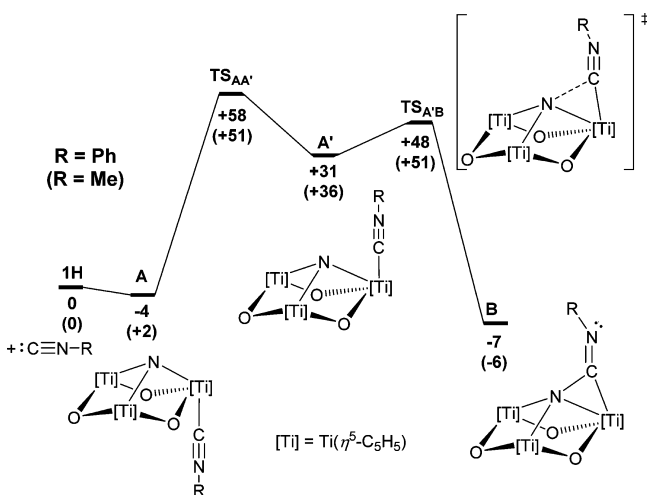
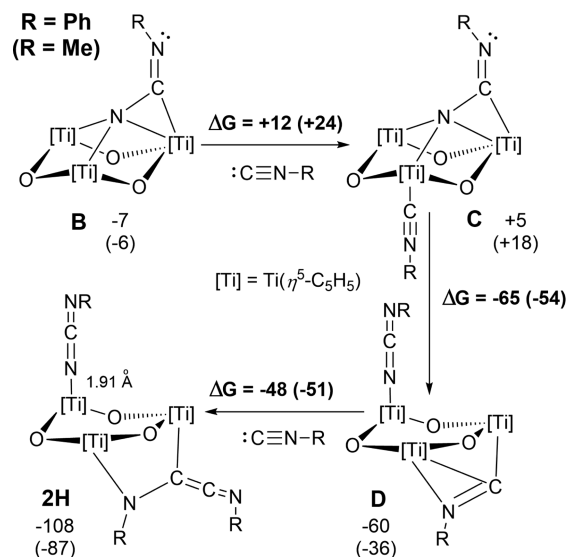


Figure 4. Gibbs free-energy profile for the incorporation of isocyanides to $[\text{Ti}(\eta^5\text{-C}_5\text{H}_5)(\mu\text{-O})_3(\mu_3\text{-N})]$ (**1H**) and carbon–nitrogen bond formation. Calculated Gibbs free energies for PhNC (and in parentheses for MeNC) in $\text{kJ}\cdot\text{mol}^{-1}$.

along the process, and [Figures 5](#) and [6](#) display the structures of selected species for the PhNC substrate, whereas the analogous species for MeNC are provided in the [Supporting Information](#). Since calculated Gibbs free energies overestimate the translational entropy loss in the associative processes, we corrected them applying Whitesides' correction¹⁶ as in the previous works of Sakaki et al.¹⁷ (see [Computational Details](#)). The incorporation of the first isocyanide molecule leads to the formation of the carbon–nitrogen bond with a low-energy requirement as illustrated in [Figure 4](#). Initially, the isocyanide can coordinate to one of the three titanium atoms through the carbon lone pair forming adduct **A**. As reported for the ammonia attack on the complex $[\text{Ti}(\eta^5\text{-C}_5\text{H}_5)(\mu\text{-O})_3(\mu_3\text{-CH})]$,⁶ in **A**, the isocyanide probably approaches the basal region of the complex **1H**, which is less hindered than the apical one. The latter isocyanide approach would yield complex **A'** (see [Figure 4](#)). Actually, the formation of complex **A** is thermodynamically favored over that of complex **A'** by 35 and 34 $\text{kJ}\cdot\text{mol}^{-1}$ for $\text{R} = \text{Ph}$, A_{Ph} , and Me , A_{Me} , respectively.³³ Nevertheless, the carbon–nitrogen formation should occur from complex **A'**, in which the isocyanido ligand is located cis with respect to the nitrido group. Complex **A'** can be formed

Scheme 3. Mechanism for the Incorporation of the Second and the Third Isocyanide Molecules to the Model Complex **1H**^a



^aCalculated Gibbs free-energy variations (ΔG) and relative energies with respect to **1H** for PhNC (and in parentheses for MeNC) in $\text{kJ}\cdot\text{mol}^{-1}$.

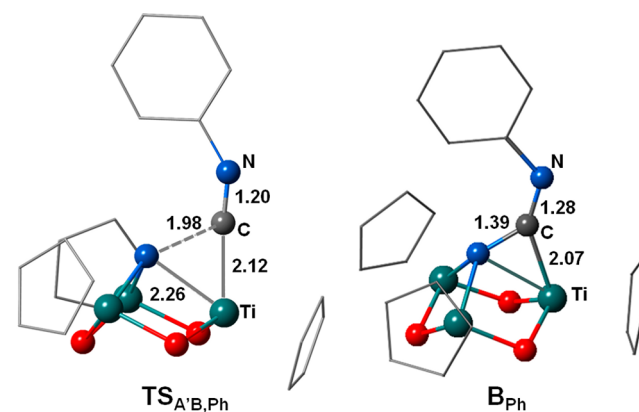


Figure 5. Computed molecular structures (\AA) of the transition state for the carbon–nitrogen bond formation ($\text{TS}_{\text{A}'\text{B},\text{Ph}}$) and the resulting intermediate (B_{Ph}).

from **A** via an intramolecular rearrangement of the isocyanido and the cyclopentadienyl (Cp) ligands that are not involved in the $\text{Ti}_3\text{O}_3\text{N}$ skeleton. Such a process has already been reported for the mentioned ammonolysis of $[\text{Ti}(\eta^5\text{-C}_5\text{H}_5)(\mu\text{-O})_3(\mu_3\text{-CH})]$,⁶ and for the acetylene addition to $[\{(\text{HCC})\text{Zn}\}(\mu_3\text{-N})(\mu_3\text{-NH})_2\{\text{Ti}(\eta^5\text{-C}_5\text{H}_5)\}_3(\mu_3\text{-N})]$,^{5d} the electronic energy barriers being moderate, 75 and 62 $\text{kJ}\cdot\text{mol}^{-1}$, respectively. Here, the computed Gibbs energy barriers are also moderate, 62 and 49 $\text{kJ}\cdot\text{mol}^{-1}$, for ligand rotation in A_{Ph} and A_{Me} , respectively. Therefore, it is reasonable to assume that the isocyanide and **1H** form first complex **A**, which then rearranges to complex **A'** (see [Figure 4](#)). Nevertheless, we cannot fully discard a mechanism in which the isocyanide coordinates directly to a Ti center cis with respect to the nitrido group.

In complex **A'**, the apical nitrido can attack the coordinated isocyanido carbon atom to form the new carbon–nitrogen bond, overcoming a very low energy barrier, 17 and 15 $\text{kJ}\cdot\text{mol}^{-1}$ for PhNC and MeNC , respectively. The corresponding

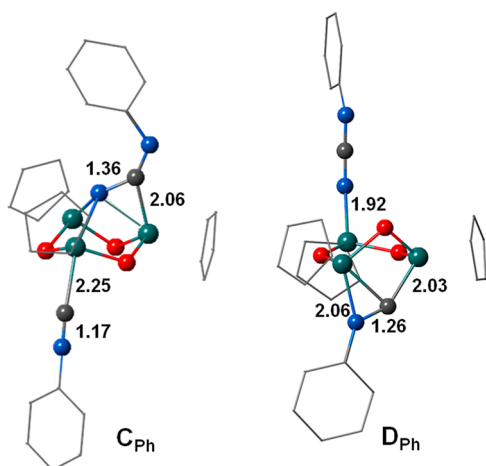


Figure 6. Computed molecular structures (Å) of two intermediate species incorporating two PhNC molecules, C_{Ph} and D_{Ph} .

transition state for the PhNC substrate, $TS_{A',B,Ph}$, is displayed in Figure 5. In the transition state $TS_{A',B,Ph}$, the distance between the isocyanide carbon and the nitride nitrogen shortens from 2.44 Å in A' to 1.98 Å, and simultaneously, the isocyanide fragment starts bending (from $C-N-Ph = 162^\circ$ in A'_{Ph} to 145° in $TS_{A',B,Ph}$).

For the titanium oxonitride complex, the active role of the apical nitrogen atom in chemical reactivity was computationally anticipated from the analysis of the frontier molecular orbitals,³⁴ as done in other transition metal oxonitrides.³⁵ In addition, the interaction of the isocyanido with the titanium center in A' elongates the $Ti-N_{apical}$ bond length and raises the energy of the occupied nitrogen p -type orbitals. This suggests an increase of nucleophilicity of the nitrido group that reacts easily with the π^* -antibonding molecular orbital of the isocyanido $C\equiv N$ bond polarized toward the carbon atom leading to complex **B** (Figure 4). Besides the nitrogen–carbon bond formation, the other significant transformation in **B** is the bending of the isocyanido fragment accompanied by $C-N$ bond lengthening ($C-N-Ph = 176^\circ$ in A_{Ph} and 125° in B_{Ph} ; $C-N = 1.17$ Å in A_{Ph} and 1.28 Å in B_{Ph}). The overall process from **1H** to **B** is exergonic by 7 and 6 $\text{kJ}\cdot\text{mol}^{-1}$ for the PhNC and MeNC substrates, respectively, complex **B** being lower in energy than **A**. The reader can notice that the differences between the species containing PhNC and MeNC are qualitatively irrelevant. Therefore, hereinafter we will focus the discussion on the results obtained for the PhNC substrate, commenting in specific cases on the differences with MeNC.

In the next step, intermediate **B** can incorporate a second isocyanide molecule via coordination to another titanium center through the carbon lone pair to give complex **C** (Scheme 3). Although the coordination is exothermic by 35 $\text{kJ}\cdot\text{mol}^{-1}$, the bimolecular process ($B + CNPh \rightarrow C$) becomes slightly endergonic, +12 $\text{kJ}\cdot\text{mol}^{-1}$, once we computed the entropy loss. Nevertheless, the ligand rearrangement from **C** to **D** is clearly exergonic, yielding species **D**, which is 60 $\text{kJ}\cdot\text{mol}^{-1}$ below reactants and provides the thermodynamic driving force for the reaction. As expected, the isocyanido coordination elongates 0.40 Å the titanium–nitrogen bond in that metal center. From **C**, the reaction proceeds through a sequence of intramolecular isocyanido rearrangements, ending in the more stable titanium complex **D** as detailed in the Supporting Information (see Scheme S1) for MeNC. In brief, we could characterize different

steps between **C** and **D**, where the computed relative electronic energies of the intermediates with respect to C_{Me} range from +26 to –24 $\text{kJ}\cdot\text{mol}^{-1}$, and the largest energy barrier is 56 $\text{kJ}\cdot\text{mol}^{-1}$. Overall, the transformation from **C** to **D** is thermodynamically favorable and occurs smoothly.

Complex **D** (Figure 6) shows a terminal Ti-carbodiimido fragment ($Ti-N = 1.92$ Å, $N-C = 1.21$ Å, $C-N = 1.24$ Å, and $C-N-Ph = 131^\circ$), similar to that of compound **2**, and an isocyanido ligand bridging two titanium centers ($Ti-N = 2.06$ Å, $N-C = 1.26$ Å, and $C-Ti = 2.03$ Å). The bridging isocyanido ligand is bent at the nitrogen atom with a $C-N-C_{Ph}$ angle of 131° that carries a lone pair to bind to the titanium center. Moreover, the isocyanido structural disposition in **D** is similar to others reported for early transition metal complexes.³⁶ The lowest unoccupied molecular orbital in D_{Ph} corresponds formally to the bridging carbon–nitrogen π -antibonding orbital with some contribution of the empty titanium d orbitals (see Figure S2 in Supporting Information). The π^*_{C-N} is polarized toward the carbon atom, explaining the approach of the third isocyanide molecule to the carbon of the bridging isocyanido and the carbon–carbon coupling between both moieties. The resulting complex, $2H_{Ph}$, is remarkably stable, the computed Gibbs free energy being –108 $\text{kJ}\cdot\text{mol}^{-1}$ with respect to **1H**. For MeNC the corresponding Gibbs free energy is less stabilizing (–87 $\text{kJ}\cdot\text{mol}^{-1}$), which could be related to the fact that a structure such as **2** was not observed for the alkyl isocyanide.

In general, the computed geometry of $2H_{Ph}$ is in good agreement with the experimental one, **2** (see Table S1 in Supporting Information for details). As suggested from the geometric parameters (see above), the analysis of the frontier molecular orbitals of $2H$ shows that the highest occupied molecular orbital (HOMO) and HOMO–1 orbitals contains a $p_\pi-d_\pi$ bonding interaction between the vacant d orbitals at the Ti centers and the occupied p -type orbitals at the two coordinated N centers (Figure 7). Thus, in both the

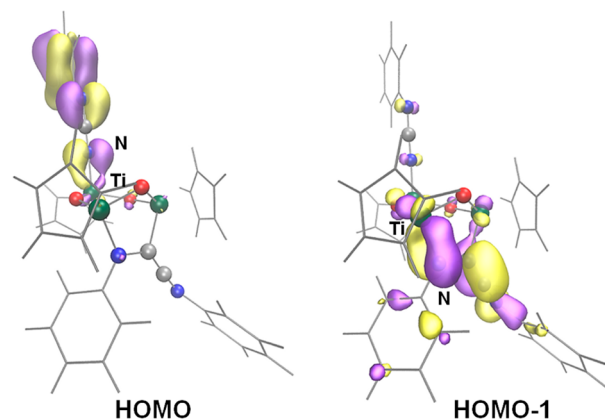
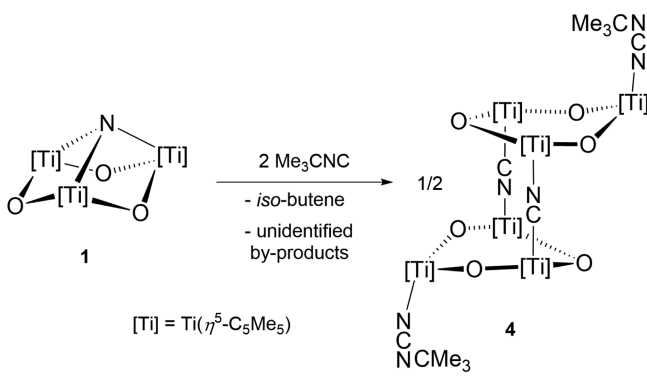


Figure 7. Representation of the $p_\pi-d_\pi$ -type orbitals HOMO and HOMO–1 for the structure $2H_{Ph}$.

carbodiimido and the heterocumulene $[ArNCCNAr]$ fragments the nitrogen is acting as a four-electron donor ligand, as previously reported for the coordination of an amido group to the same titanium molecular oxide.⁶ Thus, the negative charge supported by the nitrido group has been transferred to the $ArNCN$ and $ArNCCNAr$ ligands along the process, whereas the Ti atoms remain fully oxidized.

To further probe the scope of the C–N bonds formation with isocyanides, reaction of **1** with *t*BuNC was performed in 1:1, 1:2 ratios or excess in toluene or hexane at room temperature (see Scheme 4). Compound **4** was isolated as a

Scheme 4. Reaction of **1** with *t*BuNC



dark-green microcrystalline solid in 56% yield after 1 d. Once the crystals precipitated from toluene or hexane, they were no longer soluble in aliphatic solvents and scarcely soluble in aromatic solvents such as pyridine.

The NMR spectra of **4** revealed a paramagnetic product that room-temperature magnetization measurement by the method of Evans³⁷ gave $\mu_{\text{eff}} = 2.58 \mu_{\text{B}}$, consistent with their formulation as a complex with two unpaired electrons. Additionally, isobutene [4.719 (hept, 2H), 1.581 (t, 6H)] was identified when the reaction was monitored by ¹H NMR spectroscopy. The IR spectrum of **4** reveals bands at 2208, 2139, 2085, 1651, and 1554 cm⁻¹, which could be assigned to the cyanide²⁹ and terminal carbodiimide^{3g,21} groups.

The molecular structure of compound **4** was determined by an X-ray diffraction study performed on a single dark-green crystal obtained from the mixture reaction in toluene at room temperature (see Figure 8). This species shows a similar geometry to that found for the derivatives [$\{\text{Ti}_3(\eta^5\text{-C}_5\text{Me}_5)_3(\mu\text{-O})_4\}(\text{NCM}(\text{CO})_5)_2$] [M = Cr, Mo, W] published by our group.³⁴ As can be seen in Figure 8, the two [Ti₃O₃] rings in complex **4** are linked by linearly bridging cyanide groups, in a similar way to that reported for [Ti(η^5 -C₅H₅)₂(CN)]₄³⁸ or [Ti(η^5 -C₅H₅)₂(CN)]₃.³⁹ The pentamethylcyclopentadienyl groups attached to Ti(1) and Ti(2) complete the typical three-legged piano-stool geometry for these metal centers, while Ti(3) fills its coordination sphere also with a *tert*-butylcarbodiimide moiety.

The rupture of two of the three Ti–N bonds in complex **1** leads to [Ti₃O₃] rings with a lower tension than that observed for the starting compound,⁶ where the apical nitrogen bridges the three titanium atoms. Ti⋯Ti distances are now ~0.5 Å longer, and [Ti₃O₃] rings present a boat conformation in which the angles Ti–O–Ti are ~35° wider, being the averaged value of 135(1)° similar to those presented by other trinuclear titanium structures in which there are no other bridges between the metal atoms different from the oxygen ligands.⁴⁰ Also, the structural disposition between the plane formed by Ti(1), Ti(2), and Ti(3) and by Ti(1), Ti(2), Ti(1)a, and Ti(2)a (69.8°) is very similar to that found for the above-mentioned titanium dimeric (Cr: 70.0(1)°, Mo: 70.1(1)°, and W: 70.5(1)°),³⁴ probably due to the high steric impediment of the pentamethylcyclopentadienyl ligands.

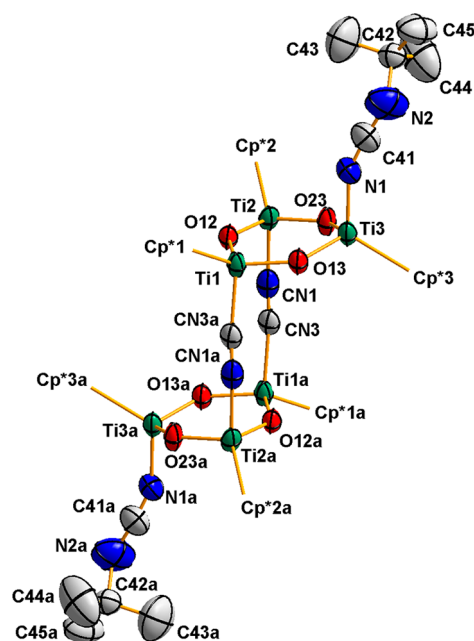


Figure 8. Ortep drawing of the molecular structure of complex **4**. Thermal ellipsoids at 50% of probability. Pentamethylcyclopentadienyl groups and hydrogen atoms were omitted for clarity. Symmetry operation (a): $-x, -y + 1, -z$. Averaged selected lengths (Å) and angles (deg): CN(1)–CN(3) 1.172(6), CN(1)–Ti(2) 2.149(8), CN(3)a–Ti(1) 2.139(7), N(1)–Ti(3) 1.983(6), C(41)–N(1) 1.139(8), C(41)–N(2) 1.306(9), C(42)–N(2) 1.455(8), Ti–O 1.802(3), CN(3)–CN(1)–Ti(2) 170.6(4), N(1)–C(41)–N(2) 171.0(7), C(41)–N(1)–Ti(3) 156.2(5), C(41)–N(2)–C(42) 125.8(6), CN(1)–CN(3)–Ti(1) 173.0(4), Ti–O–Ti 135(1), O–Ti–O 103(2).

The titanium–carbodiimido bond of 1.983(6) Å and the distances of C(41)–N(1) [1.139(8) Å] and C(41)–N(2) [1.306(9) Å] compare well with those values found for compound **2**. The N(1)–C(41)–N(2) angle of 171.0(7)° is almost linear, while the C(41)–N(2)–C(42) angle of 125.8(6)° is in agreement with an sp² hybridization for N(2).

Finally, it is important to note that the atoms of the bridging CN groups are disordered over two sites with occupancies of 0.59:0.41, as also occurred in the titanium CN-bridged complexes mentioned above.^{38,39} All Ti–CN–Ti angles are close to linear (Ti(1)–N/C–C/N 173.0(4)°, N/C–C/N–Ti(2) 170.6(4)°), and C–N bond lengths (1.172(6) Å) are similar to those described in the literature for a triple bond [C–N 1.14 Å].²⁴

The existence of these bridging cyanide groups in **4** could be originated by the rupture, in mild conditions, of the nitrogen–carbon single bond of the second molecule of *tert*-butyl isocyanide. This cleavage performed by transition metals is well-known in the literature.⁴¹ Thus, processes performed under mild conditions are the treatment of [V(η^5 -C₅Me₅)₂(CO)] with *tert*-butyl isocyanide, reported by Floriani et al.,^{41c} the reaction of [Sm(η^5 -C₅Me₅)₂(thf)₂] (thf = tetrahydrofuran) with *t*BuNC to form the trimetallic complex [Sm(η^5 -C₅Me₅)₂(CN*t*Bu)(μ -CN)]₃ published by Evans et al.,^{41h} and the reaction of *trans*-[Mo(N₂)₂(Me₈[16]aneS₄)] with *t*BuNC to afford *trans*-[Mo(CN)₂(Me₈[16]aneS₄)].⁴¹ⁱ

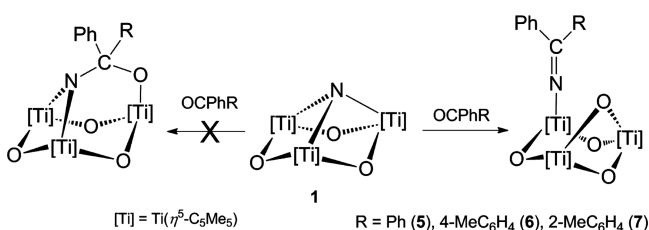
We wondered whether other unsaturated reagents could also promote the formation of carbon–nitrogen bonds on the

titanium oxonitride **1**. Thus, we performed the reactions between **1** and *p*- or *o*-methylbenzophenone.

In the first place, we scouted the treatment of the oxonitride derivative [$\{\text{Ti}(\eta^5\text{-C}_5\text{Me}_5)(\mu\text{-O})\}_3(\mu_3\text{-N})$] (**1**) with benzophenone. The process was monitored by ^1H NMR spectroscopy, and although the formation of **5** occurred smoothly at room temperature, we raised the temperature to $\sim 90^\circ\text{C}$ with the aim to shorten the reaction time. In this sense, preparative scale reactions were performed by heating at $\sim 90^\circ\text{C}$ in toluene for several days, providing the complexes **5–7** as dark-red crystalline solids in reasonable yields, soluble in common solvents, with tendency to form oils in hexane or toluene.

The ^1H NMR spectra highlighted two resonances in 2:1 ratio corresponding to the pentamethylcyclopentadienyl ligands, indicative of a C_s symmetry in solution for these compounds. Therefore, the proposal of a simple insertion process of the ketone molecule into one of the three Ti– $\mu_3\text{-N}$ bonds had to be discarded (Scheme 5, left). Finally, the X-ray structures of **6**

Scheme 5. Reaction of **1** with OCP*R* (*R* = Ph, *p*-Me(C_6H_4), *o*-Me(C_6H_4))



and **7** (see Figure 9) evidenced the formation of one ketimido fragment [$-\text{N}=\text{CPhR}$] attached to one titanium atom, while

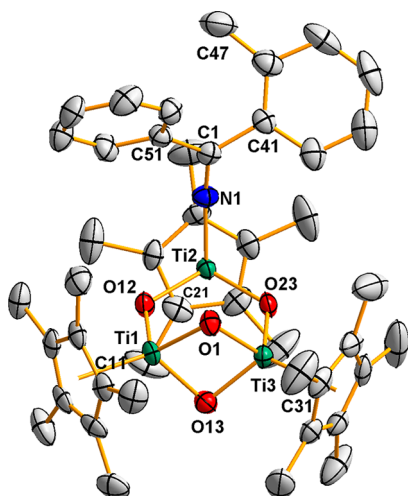


Figure 9. Ortep drawing of the molecular structure of complex **7**. Thermal ellipsoids at 50% of probability. Hydrogen atoms were omitted for clarity. Averaged selected lengths (Å) and angles (deg): C(1)–N(1) 1.271(6), N(1)–Ti(2) 1.855(4), Ti–O 1.85(2), Ti(1)⋯Ti(3) 2.673(1), Ti(2)⋯Ti 3.245(1), C(1)–N(1)–Ti(2) 165.5(4), Ti(1)–O(12)–Ti(2) 124.0(2), Ti(3)–O(23)–Ti(2) 123.6(2), Ti(3)–O–Ti(1) 92.3(1), O(12)–Ti(1)–O(1) 102.9(2), O(12)–Ti(1)–O(13) 100.7(2), O(1)–Ti(1)–O(13) 84.5(2), N(1)–Ti(2)–O(23) 106.5(2), N(1)–Ti(2)–O(12) 104.3(2), O(23)–Ti(2)–O(12) 103.5(2), O(23)–Ti(3)–O(1) 101.3(2), O(23)–Ti(3)–O(13) 102.3(2), O(1)–Ti(3)–O(13) 85.5(2).

the other two metal centers are bridged by an additional oxygen atom, as shown in Scheme 5, right.

The ^{13}C NMR spectra show the resonances for the ketimido group carbons ($>\text{C}=\text{N}$) at $\delta = 170.2$ (**5**), 170.4 (**6**), and 171.7 (**7**), in the same range as that reported for the trinuclear species [$\{\text{Ti}(\eta^5\text{-C}_5\text{Me}_5)(\mu\text{-O})\}_3(\mu\text{-CHR})(\text{N}=\text{CPh}_2)$] (*R* = H, Me).⁴² The IR spectra of **5–7** reveal $\nu(\text{N}=\text{C})$ IR frequencies around 1630–1639 cm^{-1} , which are consistent with κN -ketimido moieties.⁴³

Suitable crystals of **6** and **7** were grown from hexane solutions by slow cooling at ca. -20°C . Figure 9 shows the molecular structure of complex **7** and averaged selected distances and angles as example (data for **6** can be found in Supporting Information). The geometry of the three metal centers can be considered as a three-legged piano stool, with the pentamethylcyclopentadienyl groups located out of the $[\text{Ti}_3\text{O}_3]$ ring. However, the titanium atoms together with O(12) and O(23) form a plane, with O(13) at 1.24(1) Å below the plane, while O(1) is located at [1.26(1) Å] above it. It is noteworthy that the existence of an additional oxo bridge between two titanium atoms decreases the distance between metal centers [2.673(1) Å] with respect to the third titanium supporting the ketimido group [3.245(1) Å].

Similarly, the presence of a double oxo bridge in the structure determines the value of the Ti–O–Ti and O–Ti–O angles directly involved in the four-membered ring, with values $\sim 30^\circ$ and $\sim 15^\circ$, respectively, lower than the rest of those found in the molecule. However, these values are similar to those published for complexes that contain the $[\text{Ti}_2(\mu\text{-O})_2]$ moiety as [$\{\text{Ti}(\eta^5\text{-C}_5\text{H}_2(\text{SiMe}_3)_{3-1,2,4})\text{Cl}\}_2(\mu\text{-O})_2$] [Ti⋯Ti 2.71(1) Å, Ti–O–Ti 95.8(1) $^\circ$, O–Ti–O 84.2(1) $^\circ$]⁴⁴ or [$\{\text{Ti}_3(\eta^5\text{-C}_5\text{Me}_5)_3(\mu\text{-O})_4\}_2(\mu\text{-O})$] [Ti⋯Ti 2.6963(7) Å, Ti–O–Ti 92.4(2) $^\circ$, O–Ti–O 84.5(2) $^\circ$].⁴⁵

The carbon C(1) atom in the ketimido ligand [$(o\text{-MePh})\text{PhCN}$] shows a planar triangular environment [$\sum\alpha = 359.9^\circ$ (**7**)]. However, in this fragment the distances carbon–nitrogen [1.271(6) Å] and titanium–nitrogen [1.855(4) Å] and the Ti–N–C angles [165.5(4) $^\circ$] have similar values to those found in the literature for other ketimido titanium(IV) derivatives.^{43b,46}

We also performed additional DFT calculations to analyze the formation of carbon–nitrogen bonds using the ketone substrates. In these reagents, it is also remarkable to see the total cleavage of the very strong carbon–oxygen double bond. The rupture of C=O bonds by transition metal complexes has attracted great attention due to its extensive effect on organic chemistry.⁴⁷ Figure 10 summarizes the results for the reaction with the simplified substrate H_2CO on the model molecular oxide [$\text{Ti}(\eta^5\text{-C}_5\text{H}_5)(\mu\text{-O})\}_3(\mu_3\text{-N})$] (**1H**). As in the case of the isocyanides, in the first place, the ketone interacts with a titanium center *trans* or *cis* to the μ_3 -nitrido group forming either complex **E** or **E'**. The *trans E* isomer is 51 $\text{kJ}\cdot\text{mol}^{-1}$ lower in energy than **E'**. Intermediate **E'** is a very shallow minimum, from which the insertion of the ketone into one of the three Ti– $\mu_3\text{-N}$ bonds has very low free-energy barrier (13 $\text{kJ}\cdot\text{mol}^{-1}$), the corresponding transition state (**TS_{E'F}**) lying 66 $\text{kJ}\cdot\text{mol}^{-1}$ above reactant **1H**. Thus, the overall barrier to form the new N–C bond is mostly governed by the energy cost required to achieve the coordination of the substrate *cis* to the nitride group. Unfortunately in this case, we could not locate the ligand rearrangement transition state. However, it is reasonable to assume that this process would not be too energetically demanding, just some kilojoules per mole above **E'**, if we use as

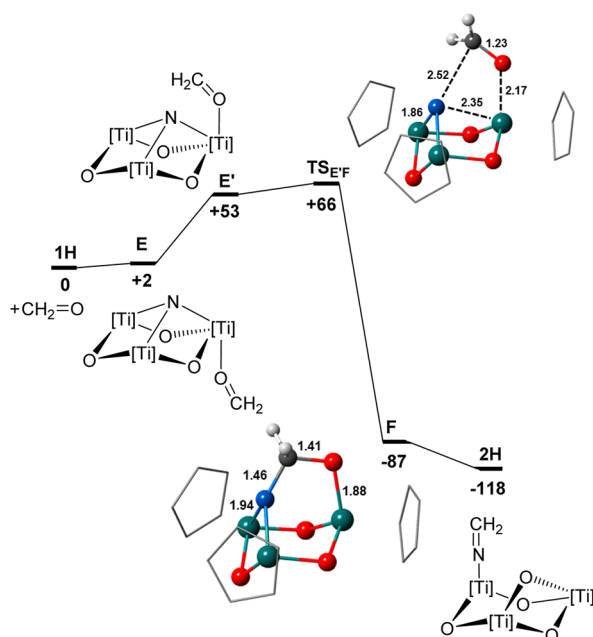


Figure 10. Gibbs free-energy profile for the reaction of $\text{H}_2\text{C}=\text{O}$ with $[\text{Ti}(\eta^5\text{-C}_5\text{H}_5)(\mu\text{-O})_3(\mu_3\text{-N})]$ (**1H**). Calculated Gibbs free energies in $\text{kJ}\cdot\text{mol}^{-1}$.

reference the energy barriers calculated for isocyanide, and previously, for amonia⁶ and acetylene.^{5d} In the resulting intermediate **F**, the new carbon–nitrogen bond formation is accompanied by partial breaking of $\text{C}=\text{O}$ bond ($\text{C}-\text{O} = 1.41 \text{ \AA}$ in **F** vs 1.22 \AA in **E** and **E'**). Structure **F** is quite stable ($-87 \text{ kJ}\cdot\text{mol}^{-1}$), but the final ketimido species, with an additional bridging oxygen, is even more stable ($-118 \text{ kJ}\cdot\text{mol}^{-1}$), the high oxophilicity of titanium being the thermodynamic driving force to yield the final product **6H**.

CONCLUSIONS

We have shown that the titanium oxonitride complex $[\text{Ti}(\eta^5\text{-C}_5\text{Me}_5)(\mu\text{-O})_3(\mu_3\text{-N})]$ (**1**) readily reacts with isocyanides and ketones to form new carbon–nitrogen bonds. As we had computationally anticipated from the analysis of the frontier molecular orbitals, the apical nitrogen atom plays an active role in the chemical reactivity of the titanium oxonitride species. Further computational studies support a mechanism involving the nucleophilic addition of the nitrido group to both isocyanide and ketone molecules. For isocyanide, the titanium complex prefers to incorporate until three isocyanide molecules. Furthermore, thermolysis of the resulted compound constitutes the first example of dearylation of an isocyanido ligand. In the case of the ketones, the high oxophilicity of titanium, combined with the nucleophilicity of the μ_3 -nitrido fragment, promotes the unusual and total cleavage of the carbon–oxygen double bond, yielding a titanium–ketimide complex, with formation of a very strong μ -oxo titanium bond.

ASSOCIATED CONTENT

Supporting Information

The Supporting Information is available free of charge on the ACS Publications website at DOI: [10.1021/acs.inorgchem.5b00943](https://doi.org/10.1021/acs.inorgchem.5b00943). CCDC 1060452–1060456 contain the supplementary crystallographic data for this paper. These data can be obtained free of charge from The Cambridge Crystallographic Data Centre via www.ccdc.cam.ac.uk/data_request/cif.

X-ray crystallographic information for compounds **1–5**. (CIF)

Computational details not included in the Article (Scheme S1, Figures S1 and S2, and Table S1). Tables containing xyz coordinates for most relevant computed structures reported in this paper. Figure S3 with ORTEP drawing for **6** and geometrical parameters. (PDF)

AUTHOR INFORMATION

Corresponding Authors

*E-mail: j.carbo@urv.cat. (J.J.C.)

*E-mail: cristina.santamaria@uah.es. (C.S.)

Notes

The authors declare no competing financial interest.

ACKNOWLEDGMENTS

We are thankful for financial support from the Spanish Ministerio de Economía y Competitividad (CTQ2013-44625-R and CTQ2011-29054-C02-01), by the Generalitat de Catalunya (2014SGR199 and XRQTC) and the Universidad de Alcalá (CCG2014/EXP-022).

DEDICATION

This paper is dedicated to Professor Rüdiger Beckhaus on the occasion of his 60th birthday.

REFERENCES

- (a) Müller, T. E.; Beller, M. *Chem. Rev.* **1998**, *98*, 675–703. and references therein. (b) *Comprehensive Organometallic Chemistry III*; Crabtree, R. H., Mingos, D. M. P., Eds.; 2007; Vol. 10, pp 101–166, 649–724. (c) Shin, K.; Kim, H.; Chang, S. *Acc. Chem. Res.* **2015**, *48*, 1040–1052.
- (a) Wolfe, J. P.; Wagaw, S.; Buchwald, S. L. *J. Am. Chem. Soc.* **1996**, *118*, 7215–7216. (b) Driver, M. S.; Hartwig, J. F. *J. Am. Chem. Soc.* **1996**, *118*, 7217–7218. (c) Palucki, M.; Wolfe, J. P.; Buchwald, S. L. *J. Am. Chem. Soc.* **1996**, *118*, 10333–10334. (d) Hartwig, J. F. *Angew. Chem.* **1998**, *110*, 2154–2177. Hartwig, J. F. *Angew. Chem., Int. Ed.* **1998**, *37*, 2046–2067. (e) Wolfe, J. P.; Wagaw, S.; Marcoux, J.-F.; Buchwald, S. L. *Acc. Chem. Res.* **1998**, *31*, 805–818. (f) Yang, B. H.; Buchwald, S. L. *J. Organomet. Chem.* **1999**, *576*, 125–146. (g) Dembech, P.; Seconi, G.; Ricci, A. *Chem. - Eur. J.* **2000**, *6*, 1281–1286. (h) Harrold, N. D.; Waterman, R.; Hillhouse, G. L.; Cundari, T. R. *J. Am. Chem. Soc.* **2009**, *131*, 12872–12873. (i) Eisenberger, P.; Schafer, L. L. *Pure Appl. Chem.* **2010**, *82*, 1503–1515. (j) Leitch, D. C.; Platel, R. H.; Schafer, L. L. *J. Am. Chem. Soc.* **2011**, *133*, 15453–15463. (k) Hanley, P. S.; Hartwig, J. F. *Angew. Chem.* **2013**, *125*, 8668–8684; *Angew. Chem., Int. Ed.* **2013**, *52*, 8510–852.
- (a) Man, W.-L.; Lam, W. W. Y.; Lau, T.-C. *Acc. Chem. Res.* **2014**, *47*, 427–439. For some original articles, see: (b) Crevier, T. J.; Mayer, J. M. *J. Am. Chem. Soc.* **1998**, *120*, 5595–5596. (c) Brown, S. N. *J. Am. Chem. Soc.* **1999**, *121*, 9752–9753. (d) Crevier, T. J.; Bennett, B. K.; Soper, J. D.; Bowman, J. A.; Dehestani, A.; Hrovat, D. A.; Lovell, S.; Kaminsky, W.; Mayer, J. M. *J. Am. Chem. Soc.* **2001**, *123*, 1059–1071. (e) Maestri, A. G.; Cherry, K. S.; Toboni, J. J.; Brown, S. N. *J. Am. Chem. Soc.* **2001**, *123*, 7459–7460. (f) Kwong, H.-K.; Man, W.-L.; Xiang, J.; Wong, W.-T.; Lau, T.-C. *Inorg. Chem.* **2009**, *48*, 3080–3086. (g) Scepaniak, J. J.; Young, J. A.; Bontchev, R. P.; Smith, J. M. *Angew. Chem.* **2009**, *121*, 3204–3206; *Angew. Chem., Int. Ed.* **2009**, *48*, 3158–3160. (h) Tran, B. L.; Pink, M.; Gao, X.; Park, H.; Mindiola, D. J. *J. Am. Chem. Soc.* **2010**, *132*, 1458–1459. (i) Semproni, S. P.; Chirik, P. J. *Organometallics* **2014**, *33*, 3727–3737.
- (4) Eikey, R. A.; Abu-Omar, M. M. *Coord. Chem. Rev.* **2003**, *243*, 83–124.

- (5) (a) Dehnicke, K.; Strähle, J. *Angew. Chem.* **1981**, *93*, 451–464; *Angew. Chem., Int. Ed. Engl.* **1981**, *20*, 413–426. (b) Dehnicke, K.; Strähle, J. *Angew. Chem.* **1992**, *104*, 978–1000; *Angew. Chem., Int. Ed. Engl.* **1992**, *31*, 955–978. (c) Dehnicke, K.; Weller, F.; Strähle, J. *Chem. Soc. Rev.* **2001**, *30*, 125–135. (d) Carbó, J. J.; Martín, A.; Mena, M.; Pérez-Redondo, A.; Poblet, J. M.; Yélamos, C. *Angew. Chem.* **2007**, *119*, 3155–3158; *Angew. Chem., Int. Ed.* **2007**, *46*, 3095–3098 and references therein.
- (6) Aguado-Ullate, S.; Carbó, J. J.; González-del Moral, O.; Martín, A.; Mena, M.; Poblet, J. M.; Santamaría, C. *Inorg. Chem.* **2011**, *50*, 6269–6279.
- (7) Farrugia, L. J. *J. Appl. Crystallogr.* **2012**, *45*, 849–854.
- (8) (a) Sheldrick, G. M. *Acta Crystallogr., Sect. A: Found. Crystallogr.* **2008**, *A64*, 112–122. (b) Sheldrick, G. M. *Acta Crystallogr.* **2015**, *C71*, 3–8.
- (9) Frisch, M. J.; Trucks, G. W.; Schlegel, H. B.; Scuseria, G. E.; Robb, M. A.; Cheeseman, J. R.; Scalmani, G.; Barone, V.; Mennucci, B.; Petersson, G. A.; Nakatsuji, H.; Caricato, M.; Li, X.; Hratchian, H. P.; Izmaylov, A. F.; Bloino, J.; Zheng, G.; Sonnenberg, J. L.; Hada, M.; Ehara, M.; Toyota, K.; Fukuda, R.; Hasegawa, J.; Ishida, M.; Nakajima, T.; Honda, Y.; Kitao, O.; Nakai, H.; Vreven, T.; Montgomery, J. A.; Peralta, J. E.; Ogliaro, F.; Bearpark, M.; Heyd, J. J.; Brothers, E.; Kudin, K. N.; Staroverov, V. N.; Kobayashi, R.; Normand, J.; Raghavachari, K.; Rendell, A.; Burant, J. C.; Iyengar, S. S.; Tomasi, J.; Cossi, M.; Rega, N.; Millam, J. M.; Klene, M.; Knox, J. E.; Cross, J. B.; Bakken, V.; Adamo, C.; Jaramillo, J.; Gomperts, R.; Stratmann, R. E.; Yazyev, O.; Austin, A. J.; Cammi, R.; Pomelli, C.; Ochterski, J. W.; Martin, R. L.; Morokuma, K.; Zakrzewski, V. G.; Voth, G. A.; Salvador, P.; Dannenberg, J. J.; Dapprich, S.; Daniels, A. D.; Farkas, Ö.; Foresman, J. B.; Ortiz, J. V.; Cioslowski, J.; Fox, D. J. *Gaussian 09*; Gaussian Inc.: Wallingford, CT, 2009.
- (10) (a) Parr, R. G.; Yang, W. *Density Functional Theory of Atoms and Molecules*; Oxford University Press: Oxford, U.K., 1989. (b) Ziegler, T. *Chem. Rev.* **1991**, *91*, 651–667.
- (11) (a) Lee, C.; Yang, C.; Parr, R. G. *Phys. Rev. B: Condens. Matter Mater. Phys.* **1988**, *37*, 785–789. (b) Becke, A. D. *J. Chem. Phys.* **1993**, *98*, 5648–5652. (c) Stephens, P. J.; Devlin, F. J.; Chabalowski, C. F.; Frisch, M. J. *J. Phys. Chem.* **1994**, *98*, 11623–11627.
- (12) Hay, P. J.; Wadt, W. R. *J. Chem. Phys.* **1985**, *82*, 270–283.
- (13) (a) Francl, M. M.; Pietro, W. J.; Hehre, W. J.; Binkley, J. S.; Gordon, M. S.; Defrees, D. J.; Pople, J. A. *J. Am. Chem. Soc.* **1982**, *77*, 3654–3665. (b) Hehre, W. J.; Ditchfield, R.; Pople, J. A. *J. Chem. Phys.* **1972**, *56*, 2257–2261. (c) Hariharan, P. C.; Pople, J. A. *Theor. Chem. Acc.* **1973**, *28*, 213–222.
- (14) (a) Antonova, N. S.; Carbó, J. J.; Kortz, U.; Kholdeeva, O. A.; Poblet, J.-M. *J. Am. Chem. Soc.* **2010**, *132*, 7488–7497. (b) Donoeva, B. G.; Trubitsina, T. A.; Antonova, N. S.; Carbó, J. J.; Poblet, J.-M.; Al-Kadamany, G.; Kortz, U.; Kholdeeva, O. A. *Eur. J. Inorg. Chem.* **2010**, *2010*, 5312–5317. (c) Jiménez-Lozano, P.; Ivanchikova, I. D.; Kholdeeva, O. A.; Poblet, J. M.; Carbó, J. J. *Chem. Commun.* **2012**, *48*, 9266–9268. (d) Skobelev, I. Y.; Zalomaeva, O. V.; Kholdeeva, O. A.; Poblet, J. M.; Carbó, J. J. *Chem.—Eur. J.* **2015**; DOI: [10.1002/chem.201501157](https://doi.org/10.1002/chem.201501157).
- (15) Mennucci, B.; Cancès, E.; Tomasi, J. *J. Phys. Chem. B* **1997**, *101*, 10506–10517.
- (16) Mammen, M.; Shakhnovich, E. I.; Deutch, J. M.; Whitesides, G. M. *J. Org. Chem.* **1998**, *63*, 3821–3830.
- (17) (a) Ishikawa, A.; Nakao, Y.; Sato, H.; Sakaki, S. *Inorg. Chem.* **2009**, *48*, 8154–8163. (b) Zeng, G.; Sakaki, S. *Inorg. Chem.* **2011**, *50*, 5290–5297. (c) Zeng, G.; Sakaki, S. *Inorg. Chem.* **2012**, *51*, 4597–4605. (d) Aono, S.; Sakaki, S. *J. Phys. Chem. B* **2012**, *116*, 13045–13062. (e) Zeng, G.; Sakaki, S.; Fujita, K.; Sano, H.; Yamaguchi, R. *ACS Catal.* **2014**, *4*, 1010–1020.
- (18) CRC *Handbook of Chemistry and Physics*, 91st ed.; Haynes, W. M., Ed.; CRC Press, Inc.: Boca Raton, FL, 2011; pp 3–282.
- (19) Bleha, T.; Gajdoš, J.; Tvaroška, I. *J. Mol. Struct.* **1980**, *68*, 189–198.
- (20) Anet, F. A. L.; Yavari, I. *Org. Magn. Reson.* **1976**, *8* (6), 327–328.
- (21) (a) Veneziani, G.; Shimada, S.; Tanaka, M. *Organometallics* **1998**, *17*, 2926–2929. (b) Schofield, A. D.; Nova, A.; Selby, J. D.; Schwarz, A. D.; Clot, E.; Mountford, P. *Chem. - Eur. J.* **2011**, *17*, 265–285.
- (22) (a) Honzicek, J.; Erben, M.; Cisarova, I.; Vinklarek, J. *Inorg. Chim. Acta* **2005**, *358*, 814–819. (b) Herrmann, H.; Lloret Fillol, J.; Wadeh, H.; Gade, L. H. *Angew. Chem.* **2007**, *119*, 8578–8582; *Angew. Chem., Int. Ed.* **2007**, *46*, 8426–8430. (c) Mindiola, D. J. *Angew. Chem.* **2008**, *120*, 1580–1583; *Angew. Chem., Int. Ed.* **2008**, *47*, 1557–1559.
- (23) Hessen, B.; Blenkins, J.; Teuben, J. H.; Helgesson, G.; Jagner, S. *Organometallics* **1989**, *8*, 830–835.
- (24) March, J.; Smith, M. B. *March's Advanced Organic Chemistry Reactions, Mechanism, and Structure*, 5th ed.; John Wiley & Sons: New York, 2001.
- (25) Martín, A.; Mena, M.; Yelamos, C.; Serrano, R.; Raithby, P. R. *J. Organomet. Chem.* **1994**, *467*, 79–84.
- (26) Santamaría, C.; Beckhaus, R.; Haase, D.; Koch, R.; Saak, W.; Strauss, I. *Organometallics* **2001**, *20*, 1354–1359.
- (27) (a) Abarca, A.; Martín, A.; Mena, M.; Raithby, P. R. *Inorg. Chem.* **1995**, *34*, 5437–5440. (b) Yu, P.; Pape, T.; Usón, I.; Said, M. A.; Roesky, H. W.; Montero, M. L.; Schmidt, H. G.; Demsar, A. *Inorg. Chem.* **1998**, *37*, 5117–5124. (c) Carbó, J. J.; González-del Moral, O.; Martín, A.; Mena, M.; Poblet, J.-M.; Santamaría, C. *Chem. - Eur. J.* **2008**, *14*, 7930–7938. (d) Carbo, J. J.; González-del Moral, O.; Martín, A.; Mena, M.; Poblet, J.-M.; Santamaría, C. *Eur. J. Inorg. Chem.* **2009**, *2009*, 643–653.
- (28) For recent works, see: (a) Garcia, J. J.; Jones, W. D. *Organometallics* **2000**, *19*, 5544–5545. (b) Garcia, J. J.; Brunkan, N. M.; Jones, W. D. *J. Am. Chem. Soc.* **2002**, *124*, 9547–9555. (c) Li, X.; Sun, H.; Yu, F.; Flörke, U.; Klein, H.-F. *Organometallics* **2006**, *25*, 4695–4697. (d) Evans, M. E.; Li, T.; Jones, W. D. *J. Am. Chem. Soc.* **2010**, *132*, 16278–16284.
- (29) (a) Thewalt, U.; Nuding, W. *J. Organomet. Chem.* **1996**, *512*, 127–130. (b) Greidanus-Strom, G.; Carter, C. A. G.; Stryker, J. M. *Organometallics* **2002**, *21*, 1011–1013.
- (30) (a) Cotton, F. A.; Schwotzer, W.; Shamsoum, E. S. *Organometallics* **1985**, *4*, 461–465. (b) Cotton, F. A.; Shamsoum, E. S. *Polyhedron* **1985**, *4*, 1727–1734. (c) Budzichowski, T. A.; Chisholm, M. H.; Folting, K.; Huffman, J. C.; Streib, W. E.; Tiedtke, D. B. *Polyhedron* **1998**, *17*, 857–867.
- (31) Pyykkö, P.; Atsumi, M. *Chem. - Eur. J.* **2009**, *15*, 12770–12779.
- (32) (a) Rottger, D.; Erker, G. *Angew. Chem.* **1997**, *109*, 840–856; *Angew. Chem., Int. Ed. Engl.* **1997**, *36*, 812–827. (b) Choukroun, R.; Cassoux, P. *Acc. Chem. Res.* **1999**, *32*, 494–502.
- (33) The isocyanide coordination to **1H** to form **A** was computed to be quite exothermic ($\Delta E = -31$ and -32 kJ·mol⁻¹ for **A_{Ph}** and **A_{Me}**) but only slightly exergonic ($\Delta G = -4$ kJ·mol⁻¹ for **A_{Ph}**) or even slightly endergonic ($\Delta G = +2$ kJ·mol⁻¹ for **A_{Me}**).
- (34) Aguado-Ullate, S.; Carbó, J. J.; González-del Moral, O.; Gómez-Pantoja, M.; Hernán-Gómez, A.; Martín, A.; Mena, M.; Poblet, J.-M.; Santamaría, C. *J. Organomet. Chem.* **2011**, *696*, 4011–4017.
- (35) Romo, S.; Antonova, N. S.; Carbó, J. J.; Poblet, J.-M. *Dalton Trans.* **2008**, 5166–5172.
- (36) (a) Röttger, D.; Pflug, J.; Erker, G.; Kotila, S.; Fröhlich, R. *Organometallics* **1996**, *15*, 1265–1267. (b) Cotton, F. A.; Daniels, L. M.; Murillo, C. A.; Wang, X. *Inorg. Chem.* **1997**, *36*, 896–901. (c) Zhang, J.; Yi, W.; Zhang, Z.; Chen, Z.; Zhou, X. *Organometallics* **2011**, *30*, 4320–4324.
- (37) (a) Evans, D. F. *J. Chem. Soc.* **1959**, 2003–2005. (b) Sur, S. K. *J. Magn. Reson.* **1989**, *82*, 169–173. (c) Szafran, Z.; Pike, R. M.; Singh, M. M. *Microscale Inorganic Chemistry. A Comprehensive Laboratory Experience*; John Wiley & Sons, 1991; pp 56–57. (d) Grant, D. H. *J. Chem. Educ.* **1995**, *72*, 39–40. (e) Girolami, G. S.; Rauchfuss, T. B.; Angelici, R. J. *Synthesis and Technique in Inorganic Chemistry. A Laboratory Manual*, 3rd ed.; University Science Books, 1999; pp 125–128. (f) Berger, S.; Braun, S. *200 and more NMR Experiments*, 3rd ed.; Wiley-VCH, 2004; pp 305–307. (g) Bain, G. A.; Berry, J. F. *J. Chem. Educ.* **2008**, *85*, 532–536.

(38) Schinnerling, P.; Thewalt, U. *J. Organomet. Chem.* **1992**, *431*, 41–45.

(39) Ruhmann, M.; Spannenberg, A.; Villinger, A.; Schulz, A.; Beweries, T. *Z. Anorg. Allg. Chem.* **2013**, *639*, 1717–1721.

(40) (a) García-Blanco, S.; Gómez-Sal, M. P.; Martínez-Carreras, S.; Mena, M.; Royo, P.; Serrano, R. *J. Chem. Soc., Chem. Commun.* **1986**, 1572–1573. (b) Troyanov, S. I.; Varga, V.; Mach, K. *J. Organomet. Chem.* **1991**, *402*, 201–207. (c) Carofiglio, T.; Floriani, C.; Sgamellotti, A.; Rosi, M.; Chiesi-Villa, A.; Rizzoli, C. *J. Chem. Soc., Dalton Trans.* **1992**, 1081–1087. (d) Andrés, R.; Galakhov, M.; Gómez-Sal, M. P.; Martín, A.; Mena, M.; Santamaría, C. *J. Organomet. Chem.* **1996**, *526*, 135–143.

(41) It is known that *tert*-butyl isocyanide complexes readily undergo a dealkylation reaction to give cyano derivatives. (a) Boyarskiy, V. P.; Bokach, N. A.; Luzyanin, K. V.; Kukushkin, V. Y. *Chem. Rev.* **2015**, *115*, 2698–2779. For some examples see: (b) Bell, A.; Lippard, S. J.; Roberts, M.; Walton, R. A. *Organometallics* **1983**, *2*, 1562–1572. (c) Gambarotta, S.; Floriani, C.; Chiesi-Villa, A.; Guastini, C. *Inorg. Chem.* **1984**, *23*, 1739–1747. (d) Bell, A.; Walton, R. A. *J. Organomet. Chem.* **1984**, *263*, 359–369. (e) Farr, J. P.; Abrams, M. J.; Costello, C. E.; Davison, A.; Lippard, S. J.; Jones, A. G. *Organometallics* **1985**, *4*, 139–142. (f) Tetrick, S. M.; Walton, R. A. *Inorg. Chem.* **1985**, *24*, 3363–3366. (g) Jones, W. D.; Kosar, W. P. *Organometallics* **1986**, *5*, 1823–1829. (h) Evans, W. J.; Drummond, D. K. *Organometallics* **1988**, *7*, 797–802. (i) Adachi, T.; Sasaki, N.; Ueda, T.; Kaminaka, M.; Yoshida, T. *J. Chem. Soc., Chem. Commun.* **1989**, 1320–1322. (j) Cabon, N.; Paugam, E.; Pétilion, F. Y.; Schollhammer, P.; Talarmin, J.; Muir, K. W. *Organometallics* **2003**, *22*, 4178–4180.

(42) Andrés, R.; Galakhov, M. V.; Gómez-Sal, M. P.; Martín, A.; Mena, M.; Morales-Varela, M. D. C.; Santamaría, C. *Chem. - Eur. J.* **2002**, *8*, 805–811.

(43) (a) Armstrong, D. R.; Henderson, K. W.; Little, I.; Jenny, C.; Kennedy, A. R.; McKeown, A. E.; Mulvey, R. E. *Organometallics* **2000**, *19*, 4369–4375. (b) Martins, A. M.; Marques, M. M.; Ascenso, J. R.; Dias, A. R.; Duarte, M. T.; Fernandes, A. C.; Fernandes, S.; Ferreira, M. J.; Matos, I.; Conceição Oliveira, M.; Rodrigues, S. S.; Wilson, C. J. *Organomet. Chem.* **2005**, *690*, 874–884.

(44) Okuda, J.; Herdtweck, E. *Inorg. Chem.* **1991**, *30*, 1516–1520.

(45) Martín, A.; Pérez-Redondo, A. *Acta Crystallogr.* **2015**, *E71*, m97.

(46) (a) Dias, A. R.; Teresa Duarte, M.; Fernandes, A. C.; Fernandes, S.; Marques, M. M.; Martins, A. M.; da Silva, J. F.; Rodrigues, S. S. *J. Organomet. Chem.* **2004**, *689*, 203–213. (b) Nomura, K.; Yamada, J.; Wang, W.; Liu, J. *J. Organomet. Chem.* **2007**, *692*, 4675–4682. (c) Ferreira, M. J.; Matos, I.; Duarte, M. T.; Marques, M. M.; Martins, A. M. *Catal. Today* **2008**, *133–135*, 647–653.

(47) (a) McMurry, J. E. *Chem. Rev.* **1989**, *89*, 1513–1524. (b) Stone, F. G. A.; West, R. *Advances in Organometallic Chemistry*; Academic Press, 1992; Vol. 34, pp 111–148. (c) Zhang, N.; Samanta, S. R.; Rosen, B. M.; Percec, V. *Chem. Rev.* **2014**, *114*, 5848–5958.